Application of the Geometric Theory of Diffraction (GTD) to Diffraction at the Edges of Loudspeaker Baffles*

R. M. BEWS AND M. J. HAWKSFORD

Department of Electronic Systems Engineering, University of Essex, Colchester CO4 3SQ, UK

The response of a loudspeaker system employing a baffle is modified by diffraction at the baffle edges. Numerical solutions are derived using a model based on the geometric theory of diffraction to examine the major features of the diffraction process. From the model it is shown that a smoother frequency and step response result, provided the drivers are placed at unequal distances from the sides of small regularly shaped baffles or if small irregularly shaped baffles are used.

0 INTRODUCTION

Most moving-coil loudspeakers use a finite baffle. Consequently an analysis of the problems caused by diffraction at the baffle edges needs consideration. This phenomenon is significant, since amplitude response fluctuations in excess of ± 5 dB can occur for particular baffle shapes.

In the late 1950s Olson [1] presented experimental data and qualitatively predicted various diffraction effects within loudspeaker systems using the geometric theory of diffraction (GTD), a theory originally proposed by Keller in 1952 [2]. This work involved the placement of multiple diffraction point sources at the diffraction edge, which resulted in secondary radiation, which subsequently interfered with the direct driver output, giving rise to frequency and phase reference irregularities. Olson concluded that an asymmetrical placement of drive units on a curved or irregularly shaped baffle offered improvements due to the randomization of the diffraction signal path lengths. Unfortunately the calculations of amplitude and phase of these diffracted rays at the baffle edge have received minimal attention. In the present paper we offer numerical solutions to this specific problem, where to the authors' knowledge a more formal and quantitative treatment has not been discussed in the context of loudspeaker systems.

* Manuscript received 1985 May 9; revised 1986 May 16.

1 DIFFRACTION MODEL

A model of acoustic diffraction at the loudspeaker baffle edges is developed, and for simplicity the following will be assumed.

1) There is only one rebated drive unit present on the baffle. Two or more can be considered by applying the law of superposition.

2) The driver acts as a point source, later to be extended to drive units with cones of finite size.

3) The baffle is constructed out of acoustically reflective material such as wood.

The development of the model commences by calculating the sound pressure on the baffle edge at E, produced by the driver located at S, as shown in Fig. 1. The acoustical reciprocity theorem [1, pp. 24–26] is then applied, which enables the interchange of points E and S. This procedure allows a virtual source to represent the diffraction edge, where its response takes full account of the baffle-edge geometry.

At a microscopic level, the loudspeaker baffle, at point E, appears as a wedge with a solid angle γ (Fig. 2). From [3] it is found that the ratio of the sound pressure produced by a point source at the apex of a wedge to that of the point source in free air is inversely proportional to 4π minus the solid angle of the wedge. Thus the sound pressure at E, P_E, is given by

$$P_E = \frac{4\pi}{4\pi - \gamma} P_{fs}|_r \tag{1}$$

where $P_{fs}|_r$ is the sound pressure at a distance r, produced by a point source in free air, that is $(A/r)\exp(-jkr)$.

Using [3] and noting that the driver is placed on a flat plane of solid angle 2π, the sound pressure P_S produced by the driver will then be

$$P_S = 2P_{fs} \ . \tag{2}$$

If the baffle were to be infinite, the sound pressure at E would be $2P_{fs}|_r$. However, the baffle ends here and the actual sound pressure is given by Eq. (1). Consequently a change in the sound pressure occurs at the edge. For example, if $\gamma = \pi$, there will be a pressure drop from $2P_{fs}|_r$ to $1.333P_{fs}|_r$ at E.

2 DIFFRACTION SOURCES

To produce the pressure change, a point source with a suitable amplitude and phase will be placed at E. This point source will be known from now on as a diffraction point source, where essentially the GTD is being applied. At the edge,

$$M_E \exp(j\theta_E) = M_I \exp(j\theta_I) + M_D \exp(j\theta_D)$$

where

$M_E \exp(j\theta_E)$ = resultant sound pressure at E
$M_I \exp(j\theta_I)$ = incident sound pressure at E, produced by driver
$M_D \exp(j\theta_D)$ = sound pressure produced by diffraction source.

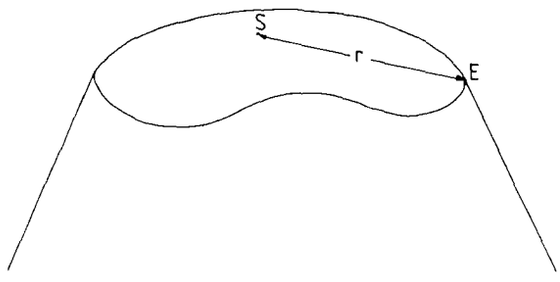

Fig. 1. Source locations on baffle.

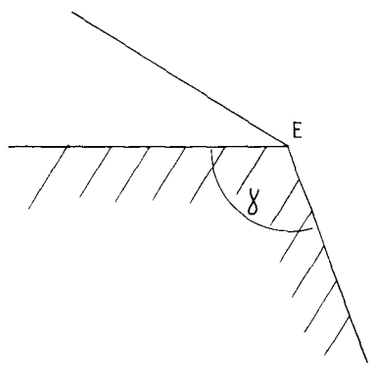

Fig. 2. Microscopic view of baffle at point E. γ—solid angle of wedge.

There is no phase difference between incident and diffracted waves, because a phase difference implies an energy loss at the edge, which cannot occur since the baffle is acoustically reflective. Most, if not all, commercially manufactured enclosures employ materials which are acoustically reflective. Hence $\theta_E = \theta_I = \theta_D$, and for convenience let them be zero. So

$$M_E = M_I + M_D \ . \tag{3}$$

If a numerical solution to this problem is to be sought, the infinite number of diffraction point sources required is impractical. As a result the total baffle edge will be quantized into N equally spaced sections, dx in length, which give rise to a finite number N of diffraction line sources. Now r becomes the average distance from the driver to a diffraction line source.

Substituting Eqs. (1) and (2) into Eq. (3) with M_D replaced by M_L as a diffraction line source is now being considered. Thus,

$$\left(\frac{4\pi}{4\pi - \gamma}\right) (\text{amplitude of } P_{fs}|_r) = 2(\text{amplitude of } P_{fs}|_r) + M_L$$

$$M_L = \left(\frac{4\pi}{4\pi - \gamma} - 2\right) (\text{amplitude of } P_{fs}|_r) \ .$$

Since the diffraction line source extends over a distance dx and the amplitude of the point source driver in free air falls as A/(radial distance), then

$$M_L = \left(\frac{4\pi}{4\pi - \gamma} - 2\right) \frac{dx}{2\pi r} A \ . \tag{4}$$

Provided dx is sufficiently small, it is acceptable to assume that the line source behaves as a point source. dx is chosen such that $(r_{max} - r_{min}) < r/1000$, since if the error $r_{max} - r_{min}$ is made even smaller, there is no detectable change in the amplitude and phase responses in the audio band from 20 Hz to 20 kHz.

3 ON-AXIS RESPONSE OF LOUDSPEAKER

3.1 Steady-State Response

Let the response of the driver at the point of observation be

$$\tilde{M}_p \exp(j\tilde{\theta}_p) \ .$$

where ~ signifies on axis, and let the response of the kth diffraction line source at the point of observation be

$$\tilde{M}_k \exp(j\tilde{\theta}_k) \ .$$

The response on axis can then be calculated by considering the interference of all the outputs from the N

diffraction line sources and the driver.

The amplitude response on axis $M_{on}(\omega)$ is given by

$$M_{on}(\omega) = \left| \tilde{M}_p \exp(j\tilde{\theta}_p) + \sum_{k=1}^{N} \tilde{M}_k \exp(j\tilde{\theta}_k) \right|$$

$$= \left| \tilde{M}_p(\cos\tilde{\theta}_p + j\sin\tilde{\theta}_p) + \sum_{k=1}^{N} \tilde{M}_k(\cos\tilde{\theta}_k + j\sin\tilde{\theta}_k) \right|$$

$$= \sqrt{\left(\tilde{M}_p\cos\tilde{\theta}_p + \sum_{k=1}^{N}\tilde{M}_k\cos\tilde{\theta}_k\right)^2 + \left(\tilde{M}_p\sin\tilde{\theta}_p + \sum_{k=1}^{N}\tilde{M}_k\sin\tilde{\theta}_k\right)^2} . \quad (5)$$

The corresponding on-axis phase response $P_{on}(\omega)$ is

$$P_{on}(\omega) = \arctan\left(\frac{\tilde{M}_p\sin\tilde{\theta}_p + \sum_{k=1}^{N}\tilde{M}_k\sin\tilde{\theta}_k}{\tilde{M}_p\cos\tilde{\theta}_p + \sum_{k=1}^{N}\tilde{M}_k\cos\tilde{\theta}_k}\right) . \quad (6)$$

The diffraction line sources will in general be farther away from the observer than the driver. Denoting the observer-to-driver distance by OBD, then on axis the distance from a diffraction line source to the observer will be $\sqrt{\mathrm{OBD}^2 + r_k^2}$ (Fig. 3). Using Eq. (4) and noting that the magnitude of the pressure is inversely proportional to the distance from the diffraction source, then at the observation point the magnitude of the response produced by the kth diffraction line source $\tilde{M}_k$ is

$$\tilde{M}_k = \frac{1}{\sqrt{\mathrm{OBD}^2 + r_k^2}} \left(\frac{4\pi}{4\pi - \gamma} - 2\right) \frac{dx}{2\pi r_k} A .$$

If $\tilde{\theta}_p$ is set to zero, making the driver response the reference, the phase of the kth diffraction line source $\tilde{\theta}_k$ will be given by

$$\tilde{\theta}_k = \frac{-\omega[r_k + (\sqrt{\mathrm{OBD}^2 + r_k^2} - \mathrm{OBD})]}{c}$$

where c is the velocity of sound.

The negative sign shows that the diffracted rays are delayed relative to the driver signal.

Using Eq. (2), the magnitude of the driver response at the observation point is given by

$$\tilde{M}_p = \frac{2A}{\mathrm{OBD}} .$$

3.2 Step Response

Let the unit step be described by $S_p(t)$. The on-axis step response is then calculated by adding the driver response to appropriately delayed diffraction line source responses. Thus the on-axis step response is given by

$$T_{on}(t) = \tilde{M}_p S_p(t) + \sum_{k=1}^{N} \tilde{M}_k S_p(t - t_k) \quad (7)$$

where

$$S_p(\tau) = 1 \text{ if } \tau > 0, \qquad \text{otherwise } S_p(\tau) = 0$$

and t_k is the time delay between the kth diffraction line source signal and the driver signal. So

$$t_k = \frac{\tilde{\theta}_k}{\omega} = \frac{r_k + (\sqrt{\mathrm{OBD}^2 + r_k^2} - \mathrm{OBD})}{c} .$$

$\tilde{\theta}_k$, $\tilde{M}_k$, and $\tilde{M}_p$ are defined in Sec. 3.1.

3.3 Steady-State and Step-Response Simulations

As an illustration the amplitude, phase, and step responses of a point source driver in the center of a 300-mm-radius circular baffle and a 600- by 600-mm square baffle have been calculated using Eqs. (5)–(7). The observer-to-driver distance OBD is 1.0 m, since most measurements are taken at this distance. Figs. 4–11 show the simulations using a DEC10 computer. All the responses are normalized to the free-air driver response, $A = 1$.

It can be seen that the amplitude and phase responses are much flatter using a square baffle instead of a circular one. This occurs because at the observer position the diffracted rays are coherent using the circular baffle,

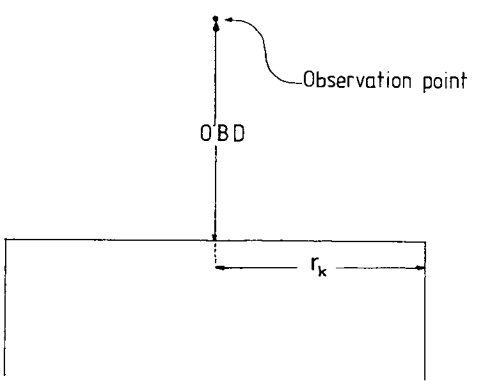

Fig. 3. On-axis geometry.

due to all the diffraction path lengths being equal, whereas for the square baffle, there is a spread of diffraction path lengths causing the diffracted rays to be less coherent. Consequently the circular baffle step response has a sharp downward transition after approximately 1 ms, when all the diffracted rays interfere with the driver signal at the same time. The downward transition in the step response using the square baffle is distributed more in time, because the diffracted rays interfere at slightly different times.

Figs. 4 and 8 can be compared with their corresponding measured responses in [1, p. 23], where there exists good experimental agreement. This suggests that the model is accurate and any slight deviations are probably due to measurement inaccuracies. The other baffle shapes described in [1] were not analyzed because of the computational complexity involved.

4 OFF-AXIS RESPONSE OF LOUDSPEAKER

When moving off axis with regard to the center of the drive unit, the path lengths of the diffracted rays

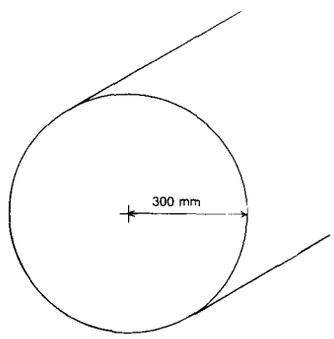

Fig. 7. Baffle shape for computer simulations of Figs. 4–6.

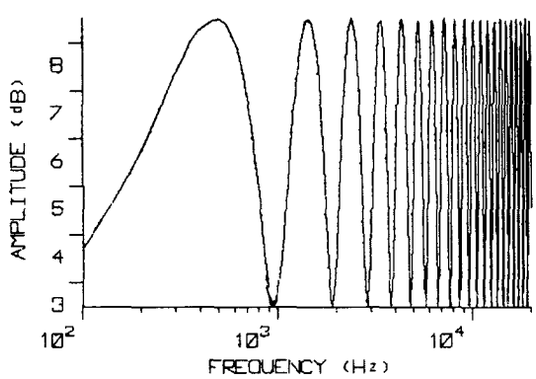

Fig. 4. On-axis amplitude response. Baffle radius 300 mm.

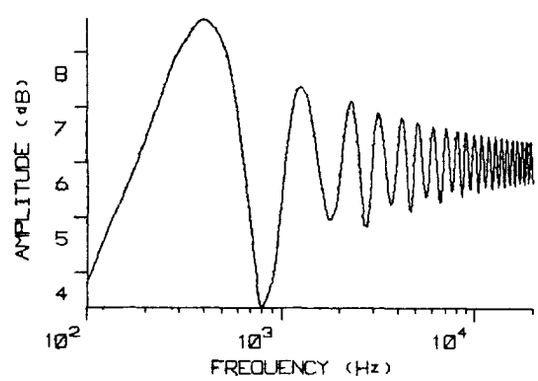

Fig. 8. On-axis amplitude response. Baffle size 600 by 600 mm.

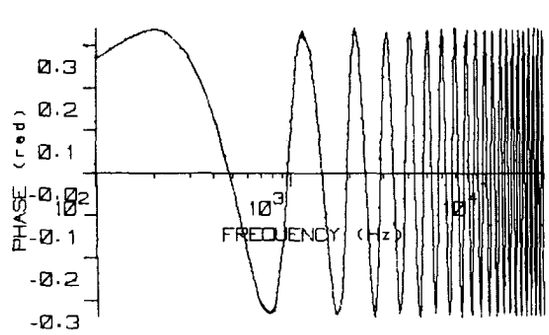

Fig. 5. On-axis phase response. Baffle radius 300 mm.

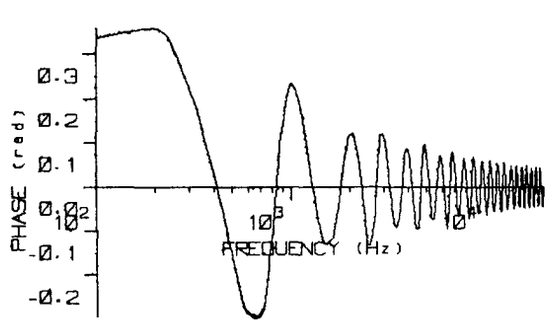

Fig. 9. On-axis phase response. Baffle size 600 by 600 mm.

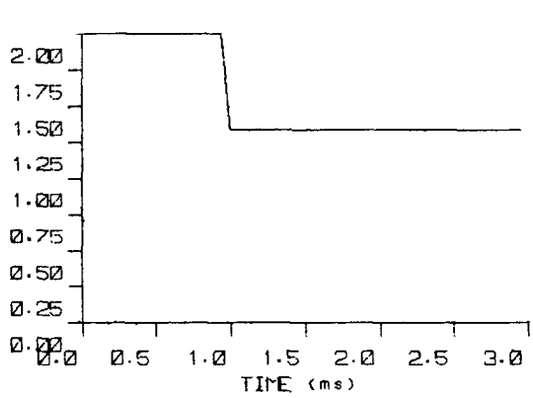

Fig. 6. On-axis step response. Baffle radius 300 mm.

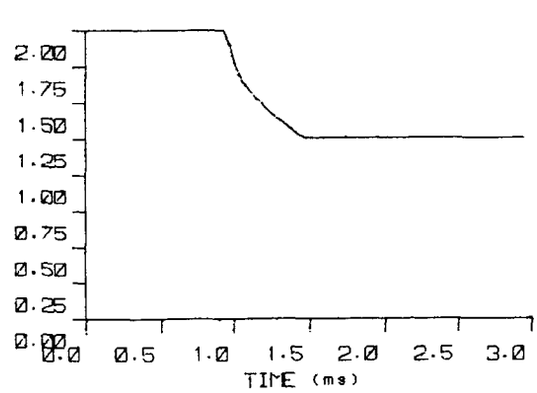

Fig. 10. On-axis step response. Baffle size 600 by 600 mm.

change. Consider the following situation in front of the baffle, as shown in Fig. 12.

Let the observer-to-driver distance be OBD, as before, the distance from the driver to the kth diffraction line source r_k, and the distance off axis OFD.

The phase difference θ_k between the driver response and the response of the kth diffraction line source becomes

$$\theta_k = \frac{-\omega[r_k + r_{OD} - \sqrt{OBD^2 + OFD^2}]}{c} \tag{8}$$

where the distance r_{OD} is shown in Fig. 12.

The corresponding time delay t_k is

$$t_k = \frac{\theta_k}{\omega} = \frac{r_k + r_{OD} - \sqrt{OBD^2 + OFD^2}}{c} . \tag{9}$$

The magnitude of the response produced by the kth diffraction line source M_k is given by

$$M_k = \frac{1}{r_{OD}} \left(\frac{4\pi}{4\pi - \gamma} - 2 \right) \frac{dx}{2\pi r_k} A \tag{10}$$

and the magnitude of the driver response M_p is

$$M_p = \frac{2A}{\sqrt{OBD^2 + OFD^2}} . \tag{11}$$

4.1 Steady-State and Step-Response Simulations

The steady-state and step responses are calculated using Eqs. (5)–(7). All these equations now use the values of θ_k, t_k, M_k, and M_p, as shown in Sec. 4.

The amplitude, phase, and step responses off axis have been computer simulated for a point source driver in the center of a 300-mm-radius circular baffle and a 600- by 6000-mm-square baffle (see Figs. 13–20). All the responses are normalized to the driver's free-air response, $A = 1$. The observer-to-driver distance OBD is set to 1.0 m and the off-axis angle [= arctan(OFD/OBD)] extends from −10° to 10°.

When off axis the diffracted rays are less coherent due to the broader distribution of path lengths. This produces flatter amplitude and phase responses and a less sharp transition around 1 ms in the step response. These changes are most noticeable using the circular baffle.

5 FINITE-SIZED DRIVERS

Since a driver has a finite diameter, which is often significant compared to the smallest dimension of the baffle, the assumption that the output from the driver

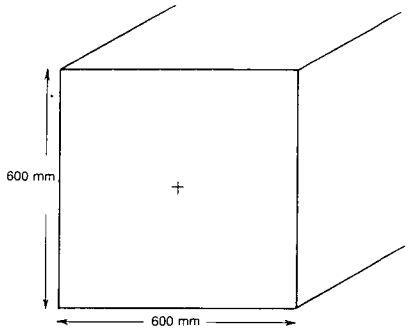

Fig. 11. Baffle shape for computer simulations of Figs. 8–10.

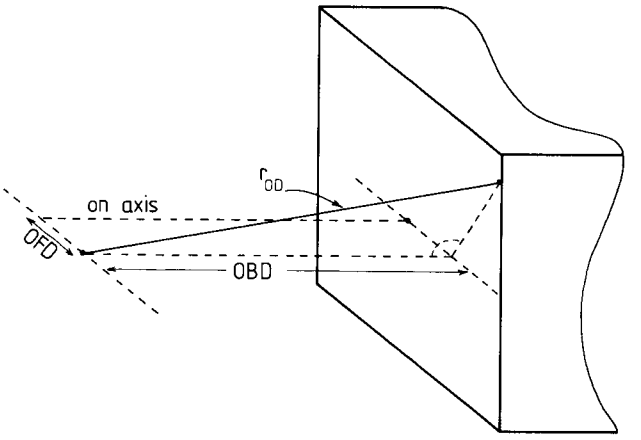

Fig. 12. Off-axis geometry.

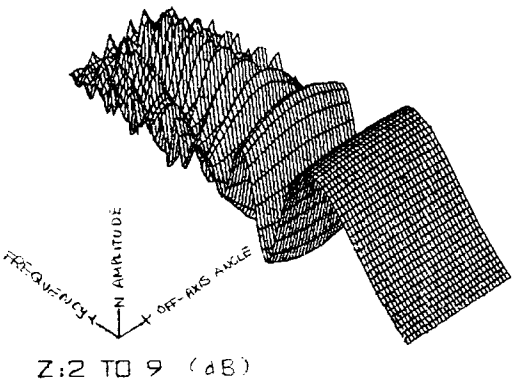

Fig. 13. Off-axis amplitude response. Baffle radius 300 mm.

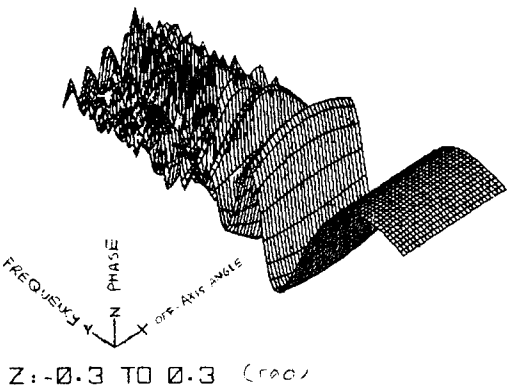

Fig. 14. Off-axis phase response. Baffle radius 300 mm.

is like that of a point source is inaccurate.

So as to approximate to the output from a flat piston drive unit, the surface of the cone is portioned into M equal area elements, each assumed to behave as a point source (see Fig. 21 for $M = 19$).

M is chosen to have the smallest allowable value, provided the amplitude and phase responses have converged in the audio band (up to 20 kHz).

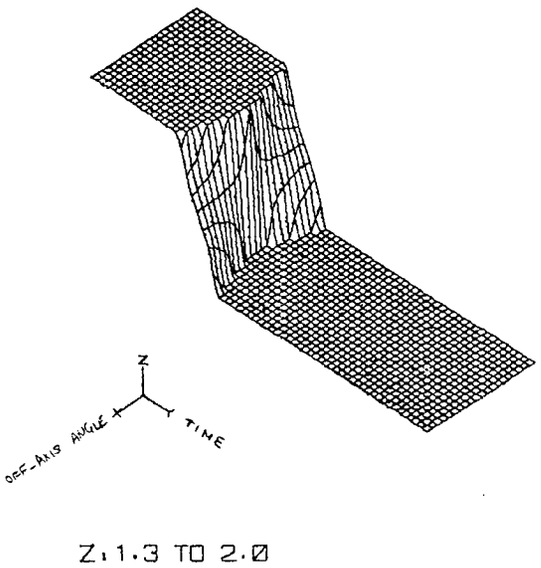

Fig. 15. Off-axis step response. Time range 0–3 ms; baffle radius 300 mm.

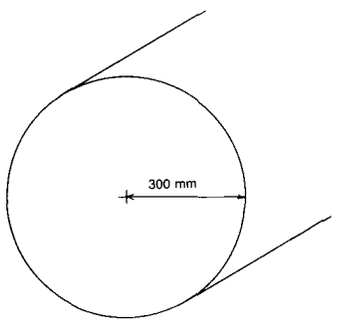

Fig. 16. Baffle shape for computer simulations of Figs. 13–15.

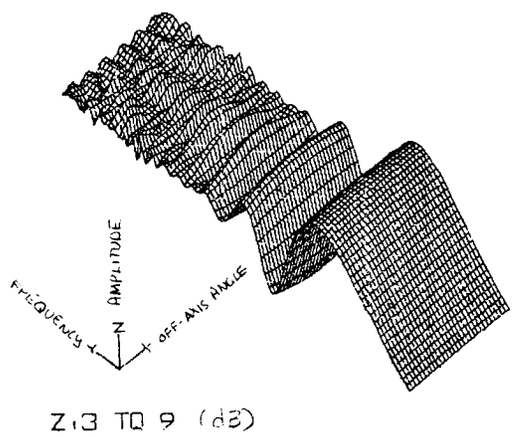

Fig. 17. On-axis amplitude response. Baffle size 600 by 600 mm.

The response of the driver on the baffle is derived by considering the interference of all the point source rays that imitate the driver and their associated diffracted rays.

5.1 On-Axis Steady-State Response

Let the Lth point source on the baffle have a response given by $AR_L(\omega) + j\,AI_L(\omega)$ at a point on axis with the center of the driver. These responses are calculated by adopting a procedure similar to the on-axis steady-state response calculations discussed in Sec. 3.1. However, it must be appreciated that all but one of the point sources which make up the driver are not on axis with the observer. Therefore a phase shift must be added to each point source response and each of the associated diffracted ray responses.

The response of the driver on a baffle $Dr(\omega)$ is then given by

$$Dr(\omega) = \frac{\sum_{L=1}^{M} [AR_L(\omega) + j\,AI_L(\omega)]}{M}.$$

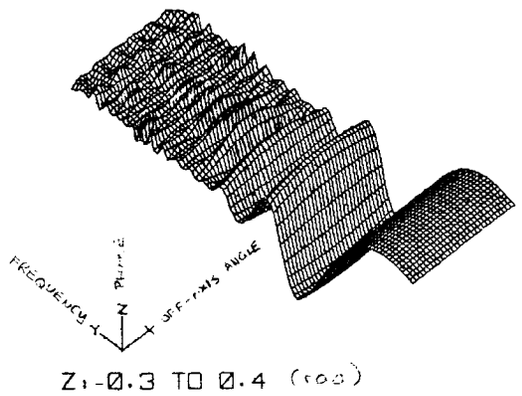

Fig. 18. Off-axis phase response. Baffle size 600 by 600 mm.

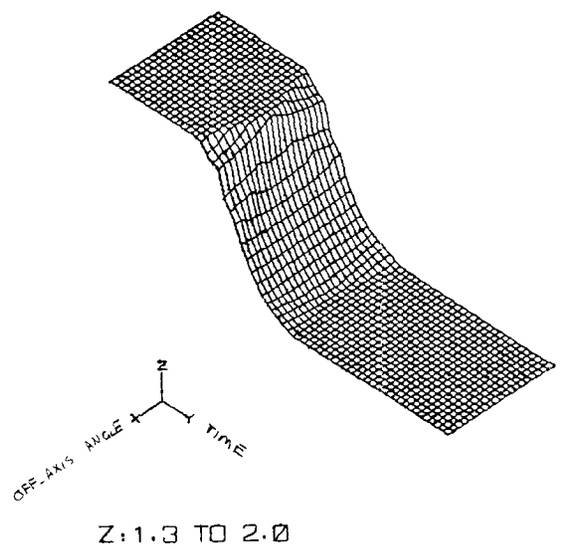

Fig. 19. Off-axis step response. Time range 0–3 ms; baffle size 600 by 600 mm.

This is then normalized to the free-air driver response, that is, Dr(ω)/free-air driver response.

Defining the response of a flat piston driver as PR(ω) + j PI(ω), (see [4] for the derivation), the on-axis normalized amplitude response $M_{con}(\omega)$ is thus

$$M_{con}(\omega) = \left| \frac{\sum_{L=1}^{M} [\mathrm{AR}_L(\omega) + \mathrm{j}\,\mathrm{AI}_L(\omega)]}{M(\mathrm{PR}(\omega) + \mathrm{j}\,\mathrm{PI}(\omega))} \right|$$

$$= \frac{\sqrt{\left[\sum_{L=1}^{M} \mathrm{AR}_L(\omega)\,\mathrm{PR}(\omega) + \sum_{L=1}^{M} \mathrm{AI}_L(\omega)\,\mathrm{PI}(\omega)\right]^2 + \left[\sum_{L=1}^{M} \mathrm{AI}_L(\omega)\,\mathrm{PR}(\omega) - \sum_{L=1}^{M} \mathrm{AR}_L(\omega)\,\mathrm{PI}(\omega)\right]^2}}{M\sqrt{\mathrm{PR}(\omega)^2 + \mathrm{PI}(\omega)^2}} . \quad (12)$$

The normalized phase response $P_{con}(\omega)$ is

$$P_{con}(\omega) = \arctan \left[\frac{\sum_{L=1}^{M} \mathrm{AI}_L(\omega)\,\mathrm{PR}(\omega) - \sum_{L=1}^{M} \mathrm{AR}_L(\omega)\,\mathrm{PI}(\omega)}{\sum_{L=1}^{M} \mathrm{AR}_L(\omega)\,\mathrm{PR}(\omega) + \sum_{L=1}^{M} \mathrm{AI}_L(\omega)\,\mathrm{PI}(\omega)} \right] . \quad (13)$$

5.2 On-Axis Step Response

Let the Lth point source on the baffle have a step response given by $\mathrm{AS}_L(t)$ at a point on axis with the center of the driver. These step responses are calculated by adopting a procedure similar to that for the on-axis step response calculation shown in Sec. 3.2. Since all but one of the point sources which imitate the driver are not on axis, a time shift must be added to their response and to the associated diffracted ray responses.

The step response of the driver on the baffle Dr(t) is then

$$\mathrm{Dr}(t) = \frac{\sum_{L=1}^{M} \mathrm{AS}_L(t)}{M} .$$

The normalized step response $T_{con}(t)$ is thus given by

$$T_{con}(t) = \frac{\mathrm{Dr}(t)}{P(t)} = \frac{\sum_{L=1}^{M} \mathrm{AS}_L(t)}{M\,P(t)} \quad (14)$$

where $P(t)$ is the step response of a flat piston driver, which can be derived by Fourier analysis of the frequency response PR(ω) + j PI(ω).

5.3 Steady-State and Step-Response Simulations

The normalized on-axis amplitude, phase, and step response simulations using Eqs. (12)–(14) for a 300-mm-radius circular baffle and a 600- by 600-mm-square baffle are shown in Figs. 22–29. The observer-to-driver distance OBD is again set to 1 m. 37 point sources are used to imitate the driver, since no discernible change occurs in any of the responses if more point sources are used.

Figs. 22, 23, 26, and 27 show the normalized am-

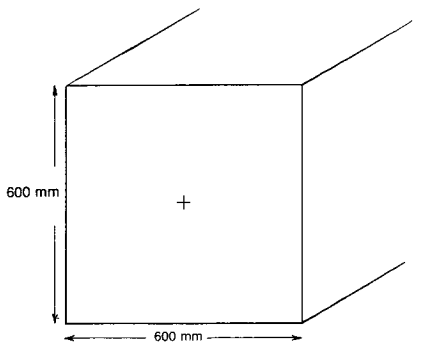

Fig. 20. Baffle shape for computer simulations of Figs. 17–19.

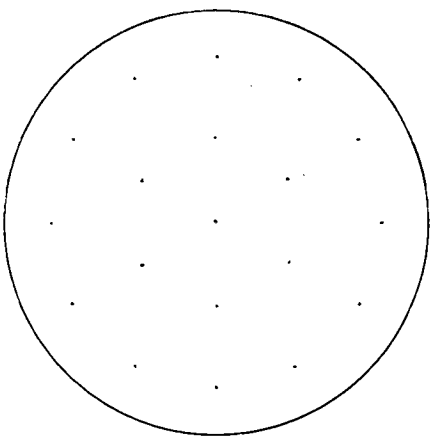

Fig. 21. Driver approximated by point sources.

plitude and phase responses for a 100-mm-radius driver, which can be compared with their corresponding responses using a point source driver as shown in Figs. 4, 5, 8, and 9. Both amplitude and phase have lower peak deviations at higher frequencies using the larger driver. This is caused by an increase in the incoherence of the diffracted rays, due to the differing locations of the point sources which imitate the driver. Consequently the step responses of Figs. 24 and 28 have a less sharp transition around 1 ms, this being most noticeable for the circular baffle. It is therefore advantageous to employ baffles that are as small as possible, ideally fractionally larger than the driver.

6 CONCLUSION

For smoother amplitude, phase, and step responses, the driver should be placed on the baffle such that the diffracted rays are as incoherent as possible. This implies that small irregularly shaped baffles should be used, or the driver located at unequal distances from the sides of small regularly shaped baffles. Rounding of the baffle edges to spatially distribute the edge should also help in this respect.

The application of sound-absorbing materials onto the baffle as first described in [5] is advantageous, since the diffracted rays will be attenuated, which subjectively improves stereo location. However, it must be appreciated that the attenuation is only significant over a limited frequency range dependent on the acoustic properties of the materials used. This will cause a drop in the amplitude response in the regions of high attenuation, leading to tonal coloration unless equalization is used.

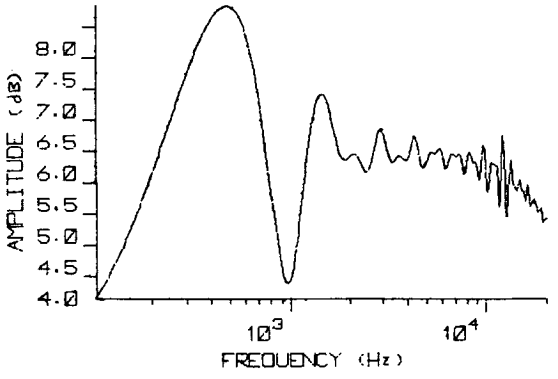

Fig. 22. On-axis amplitude response. Baffle radius 300 mm; driver radius 100 mm; 37 point sources are used.

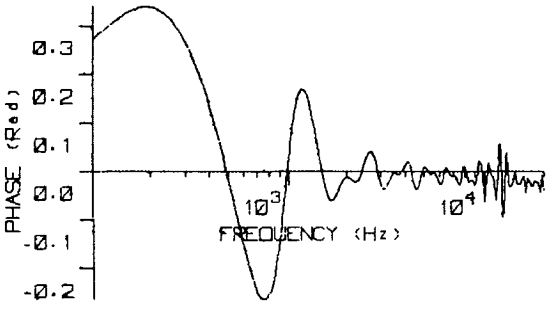

Fig. 23. On-axis phase response. Baffle radius 300 mm; driver radius 100 mm; 37 point sources are used.

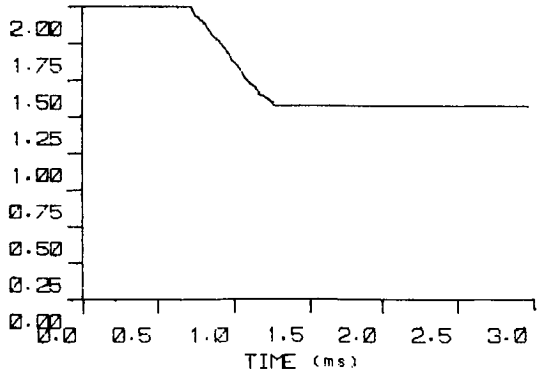

Fig. 24. On-axis step response. Baffle radius 300 mm; driver radius 100 mm; 37 point sources are used.

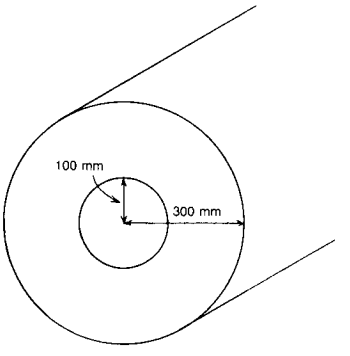

Fig. 25. Baffle shape for computer simulations of Figs. 22–24.

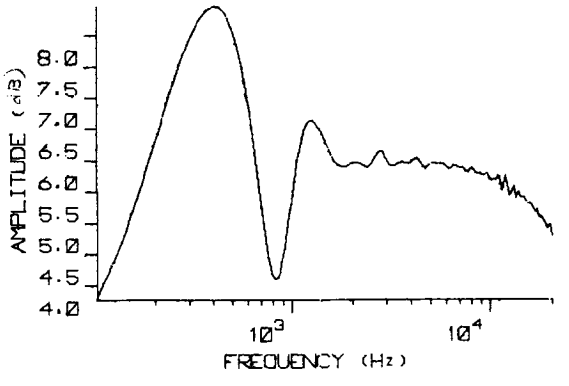

Fig. 26. On-axis amplitude response. Baffle size 600 by 600 mm; driver radius 100 mm; 37 point sources are used.

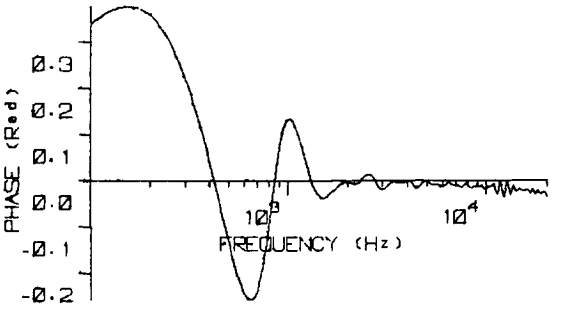

Fig. 27. On-axis phase response. Baffle size 600 by 600 mm; driver radius 100 mm; 37 point sources are used.

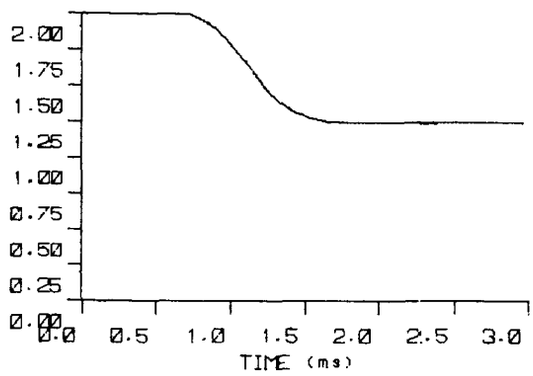

Fig. 28. On-axis step response. Baffle size 600 by 600 mm; driver radius 100 mm; 37 point sources are used.

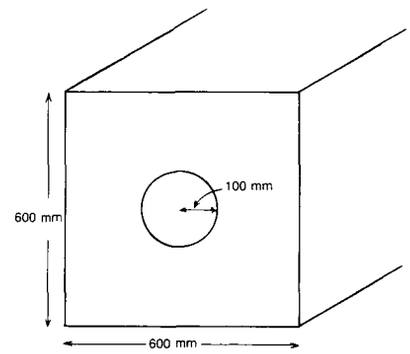

Fig. 29. Baffle shape for computer simulations of Figs. 26–28.

Diffraction is essentially a problem in the time domain, which will lend itself most easily to digital compensation. This area of research is now being actively pursued by the authors.

7 ACKNOWLEDGMENT

This work was supported by the Science and Engineering Research Council.

8 REFERENCES

[1] H. F. Olson, *Acoustical Engineering* (Van Nostrand, Princeton, NJ, 1957), chap. 1, pp. 20–24.

[2] J. B. Keller, "The Geometric Theory of Diffraction," *Symposium on Microwave Optics*, Eaton Electronics Research Laboratory, McGill University, Montreal, Canada (1953 June).

[3] Lord Rayleigh, *The Theory of Sound*, vol. 2 (Macmillan, London, 1878), sec. 280, pp. 100–102.

[4] E. Meyer and E. Neumann, *Physical and Applied Acoustics* (Academic Press, New York, 1972), chap. 5, pp. 170–177.

[5] A. Schaumberger, "Impulse Measurement Techniques for Quality Determination in Hi-Fi Equipment, with Special Emphasis on Loudspeakers," *J. Audio Eng. Soc.*, vol. 19, pp. 101–107 (1971 Feb.).

THE AUTHORS

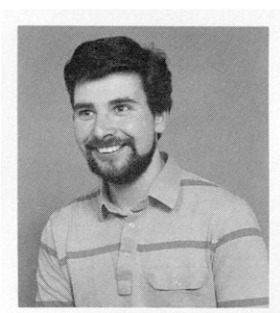

R. Bews

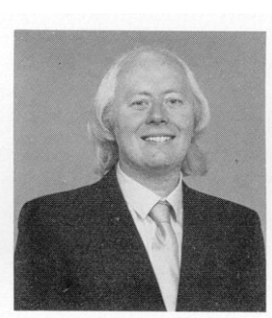

M. Hawksford

Richard Bews is currently a Ph.D. research student working within the Audio Research Group at Essex University, where his studies have included work on loudspeaker diffraction at the baffle edge and the analysis and design of crossover filters in both the analog and digital domains. Prior to his SERC-supported studentship, Bews read for a physics degree, also at Essex University, for which he gained First Class Honours in 1983. He is currently a student member of the AES.

Mr. Bews's lesiure activities also encompass audio engineering and the development of high-performance analog electronics as well as listening to music.

•

Malcolm Hawksford is presently a senior lecturer in the Department of Electronic Systems Engineering at the University of Essex, U.K., where his principal interests are in the fields of electronic circuit design and audio engineering. Dr. Hawksford studied at the University of Aston in Birmingham and gained both a First Class Honours B.Sc. and Ph.D. The Ph.D. program was supported by a BBC Research Scholarship where work on the application of delta modulation to color television was undertaken.

Since his appointment at Essex, he has established the Audio Research Group, where research on amplifier studies, digital signal processing, and loudspeaker systems has been undertaken. Dr. Hawksford has written several AES publications that include topics on error correction in amplifiers and oversampling techniques for ADC and DAC systems. His supplementary activities include designing commercial audio equipment and writing articles for *Hi-Fi News*—activities that integrate well with visits to Morocco and France. His leisure activities include listening to music, motorcycling, and motor mechanics. Dr. Hawksford is a member of the IEE, a chartered engineer, and a member of the AES.